Controlled fluorescence in a beetle's photonic structure and its sensitivity to environmentally induced changes

Mouchet, Sébastien R.; Lobet, Michaël; Kolaric, Branko; Kaczmarek, Anna M.; van Deun, Rik; Vukusic, Peter; Deparis, Olivier; Van Hooijdonk, Eloise

Published in:
Proceedings of the Royal Society B: Biological Sciences

DOI:
10.1098/rspb.2016.2334
10.1098/rspb.2016.2334

Publication date:
2016

PROCEEDINGS B

Controlled fluorescence in a beetle's photonic structure and its sensitivity to environmentally induced changes

Journal:	*Proceedings B*
Manuscript ID	RSPB-2016-2334.R1
Article Type:	Research
Date Submitted by the Author:	14-Nov-2016
Complete List of Authors:	Mouchet, Sébastien; University of Exeter, School of Physics; Universite de Namur, Department of Physics Lobet, Michaël; Universite de Namur, Department of Physics Kolaric, Branko; Universite de Namur, Department of Physics; University of Mons, Currently with Micro- and Nanophotonic Materials Group, Faculty of Science Kaczmarek, Anna; Universiteit Gent, L3 – Luminescent Lanthanide Lab, Department of Inorganic & Physical Chemistry Van Deun, Rik; Universiteit Gent, L3 – Luminescent Lanthanide Lab, Department of Inorganic & Physical Chemistry Vukusic, Pete; University of Exeter, School of Physics Deparis, Olivier; Universite de Namur, Department of Physics Van Hooijdonk, Eloise; Universite de Namur, Department of Physics
Subject:	Biophysics < BIOLOGY, Biomaterials < BIOLOGY
Keywords:	Beetle scale, Fluorescence, Natural photonic crystal, Photonic bandgap materials, Structural colour, Hoplia coerulea
Proceedings B category:	Development & Physiology

Title: **Controlled fluorescence in a beetle's photonic structure and its sensitivity to environmentally induced changes**

Authors: Sébastien R. Mouchet[1,2], Michaël Lobet[1], Branko Kolaric[1,3], Anna M. Kaczmarek[4], Rik Van Deun[4], Peter Vukusic[2], Olivier Deparis[1] and Eloise Van Hooijdonk[1]

Affiliations: [1] Department of Physics, University of Namur, Rue de Bruxelles 61, B-5000 Namur, Belgium
[2] School of Physics, University of Exeter, Stocker Road, Exeter EX4 4QL, United Kingdom
[3] Currently with Micro- and Nanophotonic Materials Group, Faculty of Science, University of Mons, Place du Parc 20, B-7000 Mons, Belgium
[4] L^3 – Luminescent Lanthanide Lab, Department of Inorganic & Physical Chemistry, Ghent University, Krijgslaan 281-S3, B-9000 Ghent, Belgium

Email addresses: s.mouchet@exeter.ac.uk, michael.lobet@unamur.be, branko.kolaric@unamur.be, anna.kaczmarek@ugent.be, rik.vandeun@ugent.be, p.vukusic@exeter.ac.uk, olivier.deparis@unamur.be, eloise.vanhooijdonk@unamur.be

Contact details of the corresponding author:

Sébastien R. Mouchet
School of Physics
University of Exeter
Physics building, Stocker Road
Exeter EX4 4QL
United Kingdom
T. +44 (0)1392 724156
s.mouchet@exeter.ac.uk

CONTROLLED FLUORESCENCE IN A BEETLE'S PHOTONIC STRUCTURE AND ITS SENSITIVITY TO ENVIRONMENTALLY INDUCED CHANGES

Sébastien R. Mouchet[1,2], Michaël Lobet[1], Branko Kolaric[1,3], Anna M. Kaczmarek[4], Rik Van Deun[4], Peter Vukusic[2], Olivier Deparis[1] and Eloise Van Hooijdonk[1]

[1] Department of Physics, University of Namur, Rue de Bruxelles 61, B-5000 Namur, Belgium

[2] School of Physics, University of Exeter, Stocker Road, Exeter EX4 4QL, United Kingdom

[3] Currently with Micro- and Nanophotonic Materials Group, Faculty of Science, University of Mons, Place du Parc 20, B-7000 Mons, Belgium

[4] L^3 – Luminescent Lanthanide Lab, Department of Inorganic & Physical Chemistry, Ghent University, Krijgslaan 281-S3, B-9000 Ghent, Belgium

The scales covering the elytra of the male *Hoplia coerulea* beetle contain fluorophores embedded within a porous photonic structure. The photonic structure controls both insect colour (reflected light) and fluorescence emission. Herein, the effects of water-induced changes on the fluorescence emission from the beetle were investigated. The fluorescence emission peak wavelength was observed to blue-shift on water immersion of the elytra whereas its reflectance peak wavelength was observed to red-shift. Time-resolved fluorescence measurements, together with optical simulations, confirmed that the radiative emission is controlled by a naturally engineered photonic bandgap while the elytra are in the dry state, whereas non-radiative relaxation pathways dominate the emission response of wet elytra.

KEYWORDS: Beetle scale; fluorescence; natural photonic crystal; photonic bandgap materials; structural colour

1. INTRODUCTION

Natural photonic structures such as those found in insects exhibit a large variety of optical properties, among which structural colours (i.e. colours due to coherent scattering)[1-3], liquid-induced colour changes[4-9] and colour sensitivity to gas or vapour[10-15] have attracted much interest. Many biological photonic structures are porous and comprise biopolymers such as

chitin, keratin and cellulose. The range of structures and optical effects found in biological systems which have been optimised through evolution for millions of years, enables the development of new designs and possible technological applications through an approach that incorporates bioinspired principles[16-19]. Another optical phenomenon found in living organisms is fluorescence emission. This phenomenon consists of a process of radiative decay (i.e. light emitting) of a substance that has previously been excited by absorption of electromagnetic radiation of higher energy. Fluorescence is found in many living organisms, terrestrial as well as aquatic, including arthropods[20,21] (e.g. butterflies[22-25], beetles[21,26], scorpions[27]), marine invertebrates (e.g. corals[28], sea anemones[29]), birds (such as parrots[30] and penguins[31]), plants[32] as well as mammals[33] (e.g. tooth enamel, white hair and nails). These organisms emit visible light and thus display colours when they are illuminated by ultraviolet (UV) light. This light emission arises due to the presence of fluorophores, such as biopterin or papilochrome II. Colour emission through fluorescence can range from blue, green, yellow to red[21] depending on the fluorophores.

The confinement of fluorophores within photonic structures can lead to controlled fluorescence, through modification of the system's density of optical states (DOS)[34-37]. When fluorescence occurs within the photonic bandgap (PhBG) of a photonic structure, a decrease in the emission intensity is observed. This arises as a consequence of the associated increase in decay time τ of the excited states[34-38]. This sort of photonic confinement can be found in several living organisms[24,25,39-48]. We note that the contribution of fluorescence emission to the colour appearance of a living organism is not always striking, often because, available solar UV intensity and insect fluorophore internal quantum efficiency can be low. This was highlighted in several *nireus* group butterflies (*Papilio bromius*, *Papilio epiphorbas*, *Papilio nireus* and *Papilio oribazus*) for which the contribution of the fluorescent blue emission to their colour is minor[25]. Fluorescence emission in living organisms is not necessarily always functional. There is no known purpose, for instance, for the fluorescence

of mammalian nails or tooth enamel. In contrast, however, the absorption of UV by fluorophores can provide insect species with protection against potential damage[1].

The male *Hoplia coerulea* (Drury 1773), a beetle from the family Scarabaeidae, exhibits a variety of optical properties including vivid iridescent colour[2,49,50], liquid- and vapour-induced colour changes[6,8,14,15,51] and fluorescence[43]. The source of all these properties lies in the flat circular scales covering the beetle's elytra. Each scale exhibits a bright blue iridescent colour[2,49,50] (Figure 1a) under incident white light due to its more or less ordered macroporous photonic structure. This structure can be described as a periodic stacked combination of thin pure cuticle layers and mixed air-cuticle porous layers[50] (Figure 1b-c). In the dry state, these give rise to a Bragg reflectance peak in the blue part of the visible spectrum (at approximately 460 nm at normal incidence). The wavelength of this peak blue-shifts as incidence angle increases. When the insect is in contact with liquids[6,8,51] or vapour[14,15], its colour reversibly changes from blue to green, as a consequence of the fluids penetrating within the photonic structure and inducing changes in refractive index contrast[6,8,14,15,51]. One interesting aspect of this fluid-induced colour change is that it takes place in a photonic structure that is not directly open to the surrounding environment[8]. An envelope encases this photonic structure and mediates fluid exchanges with the environment. Due to similarities with typical biological cells, this *H. coerulea* photonic structure was previously referred to as a "photonic cell"[8]. Moreover, fluorophores are embedded within the structure. In other work[43] it was demonstrated that the confinement of fluorescent sources in the modelled photonic structure of the scales gave rise both to enhancement and inhibition of the fluorescent emission at particular wavelengths.

Although there have been a few studies of liquid-induced fluorescence changes in insects' photonic structures, specifically relating to three butterflies (*Morpho sulkowskyi*[47], *Papilio zalmoxis*[47] and *P. nireus*[23]), the area is very much under-explored. In these previously reported studies[23,47], a liquid with a refractive index close to chitin was used to remove the effects of the photonic structure on the fluorescence steady state, by index matching.

Significant decreases in the emitted energy[47] and the decay time[23] were observed with the decrease of the refractive index contrast, while variations of the emission peak wavelength as function of refractive index change were rather small (blue-shift of less than 10 nm)[47].

In this work, changes in the fluorescence steady state of the fluorophores located in the elytra of male *H. coerulea* beetles, upon contact with water, were experimentally observed. This led to a blue-shift of the fluorescent emission from the insect structure, a feature that was previously unnoticed. The fluorescence-associated colour changed from turquoise (blue-green) to dark blue. Using several morphological and optical characterisation techniques in addition to optical simulations, this surprising response was explained in terms of water-induced changes of the photonic environment in the scales' porous structure.

2. Materials and Methods

(a) Photonic structure morphology

The morphology of the elytra was investigated using a FEI Tecnai 10 (Hillsboro, Oregon, USA) transmission electron microscope (TEM) and a FEI Nova Nanolab 200 Dual-Beam (Hillsboro, Oregon, USA) scanning electron microscope (SEM). Elytra of dead *H. coerulea* were prepared following a standard sample preparation method[52]. 100 nm-thick cross sections were ultramicrotomed and transferred onto TEM analysis grids. For SEM analysis, elytra were cut into pieces of about $5 \times 5\,\mathrm{mm}^2$ and attached to the sample mount by conducting adhesive tape. This was sputter-coated with 20 nm of platinum. The focussed-ion beam facility (FIB) on the FEI Nova Nanolab 200 Dual-Beam SEM was used to reconstruct a three dimensional representation of the scale structure (FEI Avizo 3D Software).

(b) Optical characterisation

Optical microscopy was performed using an Olympus BX61 (Tokyo, Japan) microscope, an Olympus XC50 camera and an Olympus BX-UCB visible light source (in reflection mode) or

a Lumen Dynamics X-cite Series 120PCQ (Mississauga, Ontario, Canada) UV-lamp (in fluorescence mode). Further details are available as supplementary material.

The normalised reflection spectra $R = (I - B)/(W - B)$, i.e. the ratio between the spectral intensities I and W reflected by the sample and by an Avantes WS-2 (Apeldoorn, The Netherlands) white reference, respectively, including noise corrections B, were measured using an Ocean Optics QE65Pro (Dunedin, Florida, USA) spectrophotometer connected to the microscope. The numerical aperture of the microscope objective was equal to 0.50. The use of a microspectrophotometer allowed us to analyse very small areas of the elytra comprising only a few scales (i.e. spot sizes of approximately 30 μm diameter).

Fluorescence measurements were performed using an Edinburgh Instruments (Livingston, UK) FLSP920 UV−vis−NIR spectrofluorimeter equipped with a Hamamatsu R928P (Hamamatsu City, Japan) photomultiplier-tube. The recorded time-resolved dynamics were fitted by single exponential functions. Only in the case of the dry sample within the PhBG (at 466 nm), the best fit was obtained using a double exponential function. These closest theoretical fits enabled us to determine the decay time of the fluorescence emission. Further details regarding spectrofluorimetry measurements are available as supplementary material.

The chemistry of *H. coerulea's* fluorophores has not yet been identified. Furthermore, the distribution of this pigment in the photonic structure has not yet been experimentally determined. More detailed investigations of the fluorophores are necessary and are beyond the scope of the present study.

(c) Photonic model of the beetle scale and numerical methods

The elytra of male *H. coerulea* beetles are covered by almost circular scales, composed principally of chitin. Their average diameter is approximately 80 μm and their thickness is approximately 3.5 μm. The photonic structure responsible for the specular reflection of light at these scales' surfaces is revealed by electron microscope images (Figure 1b-c). It is a

161 porous multilayer formed by the periodic stacking of thin, flat pure cuticle layers and thick
162 mixed air-cuticle porous layers (network of rods separated by air gaps).

163 Based on similar electron microscope images, Vigneron *et al*.[50] and Rassart *et al*.[6] identified
164 the geometrical parameters of the structure. In our study, we used the same photonic model
165 as was presented in the two earlier studies[6,50]. On average, 12 bilayers are found in the
166 periodic stack (Figure 1b-d). Vigneron and Rassart give the thickness of cuticle layers as
167 35 nm and the thickness of the mixed air-cuticle layers as 140 nm. Their stated width of the
168 rods is 90 nm and the air gap between two successive rods is 85 nm.

169 The refractive index n_{chitin} of cuticle material (mainly chitin) is often quoted as equal to 1.56 in
170 the visible range[53]. This average dispersionless value is a good trade-off between dispersion
171 relations found in the literature[54-56] for butterfly scales and beetle exocuticle. These relations
172 are valid only in the visible range whereas the refractive index of cuticle material in the near-
173 UV range is actually not known. As first approximation, the same refractive index value was
174 used in all our simulations from near-UV to visible ranges. In the dry state, the mixed air-
175 cuticle layers are approximated by a homogeneous material with an effective refractive index
176 n_{mixed} lying between 1 (air) and 1.56 (chitin). Using a previously reported effective medium
177 approximation[6], a value of $n_{\text{mixed}} = 1.26$ is calculated for the mixed air-cuticle layers. The
178 modelled photonic structure therefore consists of a 1D periodic stack of thin pure cuticle
179 layers and thicker effective layers (Figure 1d). In the wet state, since water ($n_{\text{water}} = 1.33$)
180 replaces air in pores, the effective refractive index becomes $n_{\text{mixed}} = 1.44$. Using an effective
181 medium approximation is justified since the photonic structure does not give rise to non zero-
182 order diffraction at visible wavelengths[50] as a result of the disorder in the orientations of the
183 rods and the small distances between them (i.e. 175 nm).

184 A conventional one-dimensional transfer-matrix (1D-TM) method approach[57] was used to
185 simulate reflectance spectra of the *H. coerulea* multilayer structure in dry and wet states.
186 This method rigorously solves Maxwell's equations in each layer of the photonic structure for

187 the propagation of electromagnetic waves through layered media. In this formalism, the
188 electromagnetic field wave is decomposed in each layer into forward and backward waves
189 propagating in the direction perpendicular to the layers. An extension of the 1D-TM
190 method[43,47] was employed in order to model light emission from the structure. This extended
191 method relies on the calculation of spectral variations in the emitted intensity, normalised
192 with respect to a source in free space. It requires light to be homogeneously emitted by a
193 single layer, in which a non-zero current density vector is included in Maxwell's equations in
194 order to represent a uniform distribution of fluorophores. For a more realistic simulation of
195 arbitrary fluorophore distribution, emission spectra were calculated with the emission source
196 located in each pure cuticle layer separately, and then averaged in order to simulate light
197 emission by the sources (fluorophores) distributed across the whole photonic structure.

198 Simulations were also performed using the finite-difference time-domain (FDTD) method[58],
199 using the MIT Electromagnetic Equation Propagation (MEEP 1.2) package[59]. Further details
200 regarding these simulations are available as supplementary material.

201 The photonic band structure and the Density Of optical States (DOS) were calculated in the
202 specific case of an infinite 1D photonic crystal based on the *H. coerulea* photonic structure
203 using a Kronig-Penney model approach and presented in ref. 60. A frequency-domain
204 method, based on an eigensolver for Maxwell's equations in a plane wave basis, was used to
205 compute the Local Density Of optical States (LDOS)[61]. The LDOS $N_{\mathrm{LDOS}}\left(\vec{r},\omega\right)$ counts the
206 available number of electromagnetic modes in which photons can be emitted at the specific
207 location of the emitting source. It depends therefore on the frequency ω and the position $\vec{r}$
208 of the emitting source in the environment but not on the propagation direction. It is known to
209 be related to the emitter decay time (according to Fermi's golden rule) by the relation:
210 $\frac{\tau_0}{\tau}=\frac{N_{\mathrm{LDOS}}\left(\vec{r},\omega\right)}{N_{\mathrm{LDOS},0}\left(\vec{r}\right)}$ where τ_0 is the decay time of one emitter located in free space, τ is the
211 decay time of the emitter and $N_{\mathrm{LDOS},0}\left(\vec{r}\right)$ is the LDOS of the emitter in free space. When

$N_{\mathrm{LDOS}}(\vec{r},\omega)$ is equal to zero, no propagation mode is available at position $\vec{r}$ and frequency ω. In this case, the decay time τ is infinite and light emission is inhibited.

The same structural model was used in all simulation methods. However, for calculations of the photonic band structure, namely DOS and LDOS, the number of bilayers was assumed to be infinite instead of equal to 12.

3. Results and Discussion

The colour displayed by the male *H. coerulea* beetle scales is violet-blue (Figure 2a) and turns to green when they are in contact with water (Figure 2b). This arises due to the filling of the scales' macropores with water[6]. This appearance change corresponds to the shift of the reflectance peak maximum from 458 nm to 525 nm (namely, a red-shift) (Figure 2c). Decreases in reflectance intensity as well as in peak reflectance width are also observed.

Under exposure to UV light, the fluorescence emission from the *H. coerulea* elytra changes from turquoise to dark blue upon contact with water (Figure 2d-e). The main features of the excitation spectrum are consistent (Figure 2f): the peak wavelength is found at 365 nm and 367 nm in the dry and wet states, respectively, and their associated full width at half maximum (FWHM) values are equal to 72 nm and 67 nm, respectively. Excitation of the fluorophores is not influenced by contact with water. This indicates that the observed liquid-induced changes do not affect the ground states of the fluorophores. However, clearly the emission spectrum of the scales is significantly modified (Figure 2f): they exhibit an immersion-mediated blue-shift from 463 nm to 446 nm ($\Delta\lambda = 17\,\mathrm{nm}$) and a decrease in FWHM from 121 nm to 105 nm. This response largely exceeds the responses measured in the cases of butterfly species (typically of less than 10 nm)[47]. Notably, the direction of the immersion-mediated change of fluorescence emission peak wavelength is opposite to that of the immersion-mediated shift of reflectance peak wavelength.

The water-induced changes in fluorescence emission were found to be reversible, a property also associated with the changes in reflectance. This infers that the fluorophores are not significantly altered chemically by exposure to water and UV under our experimental conditions. For both excitation and emission spectra, a decrease in intensity upon contact with water is observed (Figure 2f). It can be explained by, among other processes, the presence of water at the surface of the sample modifying light scattering efficiency.

If fluorophores are located in an infinite photonic crystal with a significant refractive index contrast, as well as a complete PhBG preventing emission, and provided their fluorescence efficiency is assumed to be equal to 1 (namely, the only decay process is fluorescence), they will remain in their excited states. However, in the case of a finite crystal, or one with a low refractive index contrast, the decay will be radiative with an associated decay time longer than in free space. In order to investigate the effect of the environment on the fluorescence emission further, time-resolved measurements were performed. Data from these measurements indicate that when the elytron is in the dry state and has an emission wavelength inside the PhBG (at 466 nm), the decay time τ (Table 1) is significantly longer (3.9 ns) than for a wet elytron (1.4 ns). Outside the PhBG (at 546 nm), regardless of the wet or dry state, τ is shorter (1.9 ns and 1.4 ns in the dry and wet states, respectively). In the case of the wet state, the decay time of the fluorescence emission is the same both inside and outside the PhBG. This may be partly explained by the decrease in the system's refractive index contrast that leads to an associated decrease of the fluorescence inhibition in the wet state[62]. However, combined with the experimentally measured decrease in fluorescence emission intensity, this observation clearly indicates that the wet state opens non-radiative relaxation pathways, for instance quenching processes, that in parallel decrease the effect of the optical system's PhBG on fluorescence emission. In contrast, in the dry state the presence of the PhBG strongly influences emission properties and causes an increase in fluorescence emission decay time as well as a double exponential decay. The inhibition of fluorescence emission related to the observed increase of decay time is

explained by a lack of available modes for the radiative decay of the fluorophores embedded within the photonic structure with respect to the same fluorophores in a homogeneous medium. Due to this inhibition, a redistribution of energy has hence to take place leading to non-radiative transfers to the environment[38]. The longest decay time (3.9 ns) corresponds to the real life time of the fluorophores within the photonic structure. The shortest decay time (0.79 ns) is related to non-radiative relaxations of the excited states. The time-resolved measurements of the fluorescence emission from probes embedded within colloidal photonic structures[37,38] are perfectly in agreement with these results. We observed that the decay time in the dry state is more than twice the value of the decay time in the wet state, or at a frequency outside the PhBG. This is counterintuitive if we take into account the low refractive index contrast of the materials forming the photonic structure. It is a result that may be explained at a phenomenological level by considering the curvature of the biological photonic structure: this can additionally alter the system's photonic properties and, therefore, its fluorescence emission[63,64].

In the simulated photonic band structure (Figure 3b) and related DOS (Figure 3c), first and second order PhBGs are predicted at 231 nm and 464 nm in the dry state. Despite the presence of these two PhBGs, fluorescence emission can arise because the excitation peak wavelength (Figure 2f) is located between these two PhBGs: the experimental excitation peak wavelength was measured at approximately 365 nm. Additionally, the dry sample's reflectance peak wavelength, at 45° incidence (i.e. the same angle as was used for the emission spectra measurements) was 436 nm. This reflectance peak presented a 79 nm FWHM. Furthermore, the simulated reflectance spectra (at normal incidence) in dry and wet conditions (Figure 3a) confirmed the experimentally-measured red-shift that is induced by contact with water. Namely, the calculated reflectance peak wavelength is 461 nm in the dry state and 501 nm in the wet state. The PhBGs also shift towards longer wavelengths when air is replaced by water in the macropores of the photonic structure and this is the mechanism by which the decay time of the emission at 466 nm is modified. The decreases in

290 reflectance peak intensities and FWHMs, as well as the PhBG widths (in the visible and the
291 UV ranges), are also predicted when water replaces air in the structure. These predicted
292 decreases, in addition to the changes in reflectance peak wavelength, agree with the
293 observed changes of the reflectance spectrum (Figure 2c) and previously reported
294 observations[6]. Both decreases are explained by the decrease of the effective refractive index
295 contrast $n_{\text{chitin}} / n_{\text{mixed}}$ between the layers[59] from 1.24 (dry state) to 1.08 (wet state).

296 Differences between measured and simulated spectra can be observed (e.g. in terms of
297 peak wavelengths and widths). These, in part, may arise from systematic errors associated
298 with the experimental incidence and detection angles (for instance, a 20°-incidence leads to
299 a 16-nm blue-shift of the reflectance peak position with respect to a normal incidence).
300 Furthermore, although the incident beam width is smaller than the size of the scales, the
301 beam may have not been centred on one single scale: a few sections of different scales may
302 have been analysed concurrently. Finally, the system's photonic structure is modelled as an
303 idealised perfectly periodic system even though it exhibits irregular layer interfaces,
304 inhomogeneities in refractive indices and dimensions, etc.

305 The computed $\frac{\tau_0}{\tau} = \frac{N_{\text{LDOS}}\left(\vec{r}, \omega\right)}{N_{\text{LDOS},0}\left(\vec{r}\right)}$ ratio turns out to be equal to zero inside the PhBG (e.g. at
306 466 nm) in the dry state regardless of the position of the emitter. This corresponds to an
307 infinite decay time τ, i.e. light emission is inhibited. However, in the wet state, this ratio
308 ranges from 0.66 (at the layer interfaces) and 0.86 (at the middle of the mixed air-cuticle
309 porous layers). Due to the water-induced shift of the PhBG, light can be emitted at this
310 wavelength. Outside the PhBG (i.e. at 546 nm), $\frac{\tau_0}{\tau}$ ranges from 0.6 (at the middle of the
311 mixed air-cuticle porous layers) to 0.8 (at the layer interfaces) regardless of the state (dry or
312 wet) of the modelled photonic structure. These results confirm the measured decay time
313 variations induced by contact with water. We note that this ratio cannot be calculated from
314 experimental data because the decay time τ_0 in free space of the particular fluorophores

315 embedded in the structure is unknown. In addition to the absence of defects assumed in the
316 modelled photonic structure, we mention that the measurements were not performed on a
317 single fluorescence source. Each fluorophore located in the analysis area influenced the
318 measurement.
319 Since the photonic structure controls the fluorescence emission[43,47], the emission spectrum is
320 modified by the change in refractive index within the macropores of the photonic structure. In
321 order to demonstrate this effect, two models of fluorescent sources were investigated. In both
322 models, the fluorophores were assumed to be homogeneously distributed throughout the
323 cuticular material in the photonic structure. In the first set of models, fluorophores formed a
324 uniformly planar source (emitting a uniform spectrum and located at the position of one pure
325 cuticle layer). These simulations were performed for each of the 12 pure cuticle layer
326 positions using the extended 1D-TM method and the resulting emission spectra were
327 averaged (Figure 4a). In the second model (computed using a FDTD method), fluorophores
328 were modelled by 180 point sources randomly located (according to a continuous uniform
329 distribution) across the cuticle material of structure (i.e., taking into account the filling fraction
330 of material in the pure cuticle and mixed air-cuticle porous layers) (Figure 4b). In both
331 models, the intensity emitted by the sources embedded in the structure was normalised to
332 the intensity emitted by the sources in the absence of the structure. In this way, normalised
333 values greater than unity are associated with enhancement of the fluorescence by the
334 photonic structure at the corresponding wavelengths (Figure 4). Similarly, values less than
335 unity are associated with inhibition. In principle, re-absorption can affect fluorescence,
336 especially in the case of high quantum yield fluorophores. If re-absorption (or other non-
337 radiative processes) takes place, the decay of fluorescence intensity is modified and does
338 not follow a single exponential law any more. This is not the case here outside the PhBG,
339 where the decay of fluorescence intensity was found to follow a single exponential law
340 (Figure S1). The absence of substantial overlap between fluorescence excitation and
341 emission spectra and the observation of clean, single peaked emission spectra (Figure 2f)
342 also suggest that re-absorption is negligible here. Therefore, re-absorption was not taken into

account in our simulations. In both emitted intensity spectra, a blue-shift of emission peak wavelengths (corresponding to strong enhancement of emission) occurs; the peak at 480 nm blue-shifts to 428 nm and the peak at 429 nm shifts to 416 nm in the cases of first and second models, respectively. Although both models are subject to unavoidable assumptions, it is important to observe that simulations (based on two different methods) are in qualitative agreement. It is however important to admit that a perfect match cannot be expected since the emitting sources are modelled in radically different ways. The common point is the assumed uniformity of fluorophores distribution. The qualitative agreement between simulations (Figure 4) and measurements (Figure 2f) suggests that the fluorophores are distributed throughout the photonic structure.

4. Conclusions

We investigated the male *H. coerulea* beetle that presents a broad variety of optical properties. Inside the scales that cover its elytra is a macroporous photonic architecture responsible for structural colour and fluorophores responsible for fluorescence emission. Our experiments revealed that the macroporous nature of this photonic system supports fluid-induced colour changes. *H. coerulea's* intra-scale photonic structure can be approximated by a periodic multilayer stack comprising pure cuticle layers and mixed air-cuticle porous layers. Despite this structure's PhBGs the optical system has evolved in such a way that fluorescence emission is not inhibited, i.e. excitation wavelengths do not overlap with the system's PhBGs. The influence of the system's exposure to water on its fluorescence emission was also investigated for the first time. A 17 nm water-induced blue-shift, from turquoise to dark blue, of the emission peak wavelength was measured. This contrasted to the water-induced 67 nm red-shift of the reflectance peak wavelength. These changes arise due to modification in effective refractive index following pore filling by water. An additional consequence of contact with water is the decrease of the fluorescence decay time at a wavelength inside the PhBG. In the dry state, this decay time is significantly longer inside, compared to outside, the PhBG. This is the result of the PhBG's influence on fluorescence

emission. Since, in the wet state, the decay time is the same inside and outside, the PhBG, we can conclude that quenching processes take place and non-radiative relaxation pathways dominate the emission mechanism. Simulations of light emission from the system indicated that the presence of water in the macropores of the photonic structure leads to a blue-shift of the emission spectrum. This agrees with experimental data for the system. The simulations additionally confirmed the likelihood of a homogeneous distribution of fluorophores across the structure and the role of the multilayer in this water-induced change in fluorescence emission. Such a photonic system offers a new possibility to design novel functional optical materials and coatings in technological areas such as imaging, lighting, biosensing and solar cells.

DATA ACCESSIBILITY.

Data available from the Dryad Digital Repository: http://dx.doi.org/10.5061/dryad.sm72f.

COMPETING INTERESTS.

We declare we have no competing interests.

AUTHORS' CONTRIBUTIONS.

S.R.M., M.L. and E.V.H. conceived the original project. S.R.M. performed the morphological characterisation. S.R.M. and E.V.H. conducted the optical and fluorescence microscopy analyses as well as the reflectance measurements. A.M.K. and S.R.M. performed the fluorescence measurements. B.K. and S.R.M. performed the time-resolved fluorescence data analysis. S.R.M. performed the LDOS simulations and M.L., the FDTD method simulations. E.V.H. and S.R.M. performed the 1D-TM method simulations as well as the calculation of the photonic band structures and related DOS. S.R.M., M.L., B.K., A.M.K., R.V.D., P.V., O.D. and E.V.H. discussed the results. S.R.M., M.L. and E.V.H. wrote the manuscript with input from B.K., P.V. and O.D. All authors commented on the manuscript and gave approval to its final version.

ACKNOWLEDGEMENTS.

The authors thank Louis Dellieu (Department of Physics, UNamur) for technical support during the collection of samples and Michaël Sarrazin (Department of Physics, UNamur) for commenting an early version of this article as well as for fruitful discussions. This research used resources of the "Plateforme Technologique de Calcul Intensif (PTCI)", UNamur (http://www.ptci.unamur.be), which is supported by F.R.S.-FNRS under the convention No. 2.4520.11 as well as of the Electron Microscopy Service (SME), UNamur (http://www.unamur.be/en/sevmel). PTCI and SME are members of the "Consortium des Équipements de Calcul Intensif (CÉCI)" (http://www.ceci-hpc.be) and of the "Plateforme Technologique Morphologie – Imagerie" (UNamur), respectively.

FUNDING.

S. R. Mouchet was supported by the Belgian National Fund for Scientific Research (F.R.S.-FNRS) as a Research Fellow and by Wallonia-Brussels International (WBI) through a Postdoctoral Fellowship for Excellence program WBI.WORLD. B. Kolaric acknowledges financial support from the "Action de Recherche Concertée" (BIOSTRUCT project – No.10/15-033) of UNamur, from Nanoscale Quantum Optics COST-MP1403 action and from F.R.S.-FNRS; Interuniversity Attraction Pole: Photonics@be (P7-35, Belgian Science Policy Offfice). A. M. Kaczmarek acknowledges Ghent University's Special Research Fund (BOF) for a Postdoctoral Mandate (project BOF15/PDO/091). R. Van Deun thanks the Hercules Foundation (project AUGE/09/024 "Advanced Luminescence Setup") for funding. E. Van Hooijdonk was supported by F.R.S.-FNRS as a Postdoctoral Researcher. This research was also supported by F.R.S.-FNRS through the Researchers' Credit CC 1.5075.11F and the Research Credit CDR J.0035.13.

REFERENCES

1. Berthier S. 2000 La couleur des papillons ou l'impérative beauté - Propriétés optiques des ailes de papillons. Springer, Paris.
2. Berthier S. 2003 Iridescences, les couleurs physiques des insects. Springer, Paris.

3. Kinoshita S. 2008 Structural Colors in the Realm of Nature. World Scientific Publishing Co, Singapore.

4. Vigneron JP, Pasteels JM, Windsor DM, Vértesy Z, Rassart M, Seldrum T, Dumont J, Deparis O, Lousse V, Biró LP *et al*. 2007 Switchable reflector in the Panamanian tortoise beetle *Charidotella egregia* (Chrysomelidae: Cassidinae). Phys. Rev. E 76, 031907. (doi:10.1103/PhysRevE.76.031907)

5. Rassart M, Colomer JF, Tabarrant T, Vigneron JP. 2008 Diffractive hygrochromic effect in the cuticle of the hercules beetle *Dynastes hercules*. New J. Phys. 10, 033014. (doi:10.1088/1367-2630/10/3/033014)

6. Rassart M, Simonis P, Bay A, Deparis O, Vigneron JP. 2009 Scales coloration change following water absorption in the beetle *Hoplia coerulea* (Coleoptera). Phys. Rev. E 80, 031910. (doi:10.1103/PhysRevE.80.031910)

7. Liu F, Dong BQ, Liu XH, Zheng YM, Zi J. 2009 Structural color change in longhorn beetles *Tmesisternus isabellae*. Opt. Express 17, 16183-16191. (doi:10.1364/OE.17.016183)

8. Mouchet SR, Van Hooijdonk E, Welch VL, Louette P, Colomer JF, Su BL, Deparis O. 2016 Liquid-induced colour change in a beetle: the concept of a photonic cell. Sci. Rep. 6, 19322. (doi:10.1038/srep19322)

9. Wang W, Zhang W, Fang X, Huang Y, Liu Q, Gu J, Zhang D. 2014 Demonstration of higher colour response with ambient refractive index in *Papilio blumei* as compared to *Morpho rhetenor*. Sci. Rep. 4, 5591. (doi:10.1038/srep05591)

10. Potyrailo RA, Ghiradella H, Vertiatchikh A, Dovidenko K, Cournoyer JR, Olson E. 2007 *Morpho* butterfly wing scales demonstrate highly selective vapour response. Nat. Photonics 1, 123-128. (doi:10.1038/nphoton.2007.2)

11. Biró LP, Kertész K, Vértesy Z, Bálint Zs. 2008 Photonic nanoarchitectures occurring in butterfly scales as selective gas/vapor sensors. Proc. SPIE 7057, 705706. (doi:10.1117/12.794910)

12. Mouchet S, Deparis O, Vigneron JP. 2012 Unexplained high sensitivity of the reflectance of porous natural photonic structures to the presence of gases and vapours in the atmosphere. Proc. SPIE 8424, 842425. (doi:10.1117/12.921784)

13. Potyrailo RA, Starkey TA, Vukusic P, Ghiradella H, Vasudev M, Bunning T, Naik RR, Tang Z, Larsen M, Deng T *et al*. 2013 Discovery of the surface polarity gradient on iridescent *Morpho* butterfly scales reveals a mechanism of their selective vapor response. P. Natl Acad. Sci. USA 110, 15567-15572. (doi:10.1073/pnas.1311196110)

14. Mouchet S, Su BL, Tabarrant T, Lucas S, Deparis O. *Hoplia coerulea*, a porous natural photonic structure as template of optical vapour sensor. 2014 Proc. SPIE 9127, 91270U. (doi:10.1117/12.2050409)

15. Mouchet SR, Tabarrant T, Lucas S, Su BL, Vukusic P, Deparis O. Vapor sensing with a natural photonic cell. Opt. Express 24, 12267-12280. (doi:10.1364/OE.24.012267)

16. Biró LP, Vigneron JP. 2011 Photonic nanoarchitectures in butterflies and beetles: valuable sources for bioinspiration. Laser Photonics Rev. 5, 27-51. (doi:10.1002/lpor.200900018)

17. Kim JH, Moon JH, Lee SY, Park J. 2010 Biologically inspired humidity sensor based on three-dimensional photonic crystals. Appl. Phys. Let. 97, 103701. (doi:10.1063/1.3486115)

18. Ghazzal MN, Deparis O, De Coninck J, Gaigneaux EM. 2013 Tailored refractive index of inorganic mesoporous mixed-oxide Bragg stacks with bio-inspired hygrochromic optical properties. J. Mater. Chem. C 1, 6202-6209. (doi:10.1039/c3tc31178c)

19. Deparis O, Ghazzal MN, Simonis P, Mouchet SR, Kebaili H, De Coninck J, Gaigneaux EM, Vigneron JP. 2014 Theoretical condition for transparency in mesoporous layered optical media: Application to switching of hygrochromic coatings. Appl. Phys. Lett. 104, 023704. (doi:10.1063/1.4862658)

20. Lawrence RF. 1954 Fluorescence in arthropoda. J. Ent. Soc. South Africa 17, 167-170.

21. Welch VL, Van Hooijdonk E, Intrater N, Vigneron JP. 2012 Fluorescence in insects. Proc. SPIE 8480, 848004. (doi:10.1117/12.929547)

22. Cockayne EA. 1924 I. The Distribution of Fluorescent Pigments in Lepidoptera. T. Roy. Ent. Soc. London 72, 1-19. (doi:10.1111/j.1365-2311.1924.tb03347.x)

23. Vukusic P, Hooper I. 2005 Directionally Controlled Fluorescence Emission in Butterflies. Science 310, 1151. (doi:10.1126/science.1116612)

24. Trzeciak TM, Wilts BD, Stavenga DG, Vukusic P. 2012 Variable multilayer reflection together with long-pass filtering pigment determines the wing coloration of papilionid butterflies of the *nireus* group. Opt. Express 20, 8877-8890. (doi:10.1098/rsfs.2011.0082)

25. Wilts BD, Trzeciak TM, Vukusic P, Stavenga DG. 2012 Papiliochrome II pigment reduces the angle dependency of structural wing colouration in *nireus* group papilionids. J. Exp. Biol. 215, 796-805. (doi:10.1242/jeb.060103)

26. Israelowitz M, Rizvi SHW, von Schroeder HP. 2007 Fluorescence of the “fire-chaser” beetle, *Melanophila acuminate*. J. Lumin. 126, 149-154. (doi:10.1016/j.jlumin.2006.06.017)

27. Pavan M, Vachon M. 1954 Sur l'existence d'une substance fluorescente dans les téguments des Scorpions (Arachnides). C. R. Acad. Sci. Paris 239, 1700-1702.

28. Catala-Stucki R. 1959 Fluorescence Effects from Corals irradiated with Ultra-Violet Rays. Nature 183, 949. (doi:10.1038/183949a0)

29. Phillips CES. 1927 Fluorescence of Sea Anemones. Nature 119, 747. (doi:10.1038/119747c0)

30. Arnold KE, Owens IPF, Marshall NJ. 2002 Fluorescent Signaling in Parrots. Science 295, 92. (doi:10.1126/science.295.5552.92)

31. McGraw KJ, Toomey MB, Nolan PM, Morehouse NI, Massaro M, Jouventin P. 2007 A description of unique fluorescent yellow pigments in penguin feathers. Pigm. Cell Res. 20, 301-304. (doi:10.1111/j.1600-0749.2007.00386.x)

32. Goodwin RH. Fluorescent substances in plants. 1953 Annu. Rev. Plant. Physiol. 4, 283-304. (doi:10.1146/annurev.pp.04.060153.001435)

33. Tani K, Watari F, Uo M, Morita M. 2004 Fluorescent Properties of Porcelain-Restored Teeth and Their Discrimination. Mater. Trans. 45, 1010-1014. (doi:10.2320/matertrans.45.1010)

34. Purcell EM. Spontaneous emission probabilities at radio frequencies. 1946 Phys. Rev. 69, 681. (doi:10.1103/PhysRev.69.674.2)

35. Yablonovitch E. 1987 Inhibited Spontaneous Emission in Solid-State Physics and Electronics. Phys. Rev. Lett. 58, 2059-2062. (doi:10.1103/PhysRevLett.58.2059)

36. John S. 1987 Strong Localization of Photons in Certain Disordered Dielectric Superlattices. Phys. Rev. Lett. 58, 2486-2489. (doi:10.1103/PhysRevLett.58.2486)

37. González-Urbina L, Pérez-Moreno J, Clays K, Kolaric B. 2016 Phosphorescence emission from BAlq by forced intersystem crossing in a colloidal photonic crystal, Mol. Phys. 114, 2248-2252. (doi:10.1080/00268976.2016.1194495)

38. González-Urbina L, Baert K, Kolaric B, Pérez-Moreno J, Clays K. 2012 Linear and Nonlinear Optical Properties of Colloidal Photonic Crystals. Chem. Rev. 112, 2268-2285. (doi:10.1021/cr200063f)

39. Kumazawa K, Tanaka S, Negita K, Tabata H. 1994 Fluorescence from Wing of *Morpho sulkowskyi* Butterfly. Jpn. J. Appl. Phys. 33, 2119-2122. (doi:10.1143/JJAP.33.2119)

40. Lawrence C, Vukusic P, Sambles R. 2002 Grazing-incidence iridescence from a butterfly wing. Appl. Optics 41, 437-441. (doi:10.1364/AO.41.000437)

41. Vigneron JP, Kertész K, Vértesy Z, Rassart M, Lousse V, Bálint Zs, Biró LP. 2008 Correlated diffraction and fluorescence in the backscattering iridescence of the male butterfly *Troides magellanus* (Papilionidae). Phys. Rev. E 78, 021903. (doi:10.1103/PhysRevE.78.021903)

42. Van Hooijdonk E, Barthou C, Vigneron JP, Berthier S. 2011 Detailed experimental analysis of the structural fluorescence in the butterfly *Morpho sulkowskyi* (Nymphalidae). J. Nanophotonics 5, 053525. (doi:10.1117/1.3659147)

43. Van Hooijdonk E, Berthier S, Vigneron JP. 2012 Bio-inspired approach of the fluorescence emission properties in the scarabaeid beetle *Hoplia coerulea* (Coleoptera): Modeling by transfer-matrix optical simulations. J. Appl. Phys. 112, 114701. (doi:10.1063/1.4768896)

44. Van Hooijdonk E, Vandenbem C, Berthier S, Vigneron JP. 2012 Bi-functional photonic structure in the *Papilio nireus* (Papilionidae): modeling by scattering-matrix optical simulations. Opt. Express 20, 22001-22011. (doi:10.1364/OE.20.022001)

45. Van Hooijdonk E, Barthou C, Vigneron JP, Berthier S. 2012 Angular dependence of structural fluorescent emission from the scales of the male butterfly *Troïdes magellanus* (Papilionidae). J. Opt. Soc. Am. B 29, 1104-1111. (doi:10.1364/JOSAB.29.001104)

46. Van Hooijdonk E, Berthier S, Vigneron JP. 2012 Contribution of both the upperside and the underside of the wing on the iridescence in the male butterfly *Troïdes magellanus* (Papilionidae). J. Appl. Phys. 112, 074702. (doi:10.1063/1.4755796)

47. Van Hooijdonk E. 2012 Etude théorique et expérimentale de la fluorescence de structures photoniques naturelles. Ph.D. thesis - Facultés Universitaires Notre-Dame de la Paix (FUNDP) and Université Pierre et Marie Curie (Paris VI), Namur & Paris.

48. Van Hooijdonk E, Barthou C, Vigneron JP, Berthier S. 2013 Yellow structurally modified fluorescence in the longhorn beetles *Celosterna pollinosa sulfurea* and *Phosphorus virescens* (Cerambycidae). J. Lumin. 136, 313-321. (doi:10.1016/j.jlumin.2012.12.022)

49. Mason CW. 1927 Structural Colors in Insects. II. J. Phys. Chem. 31, 321-354. (doi:10.1021/j150273a001)

50. Vigneron JP, Colomer JF, Vigneron N, Lousse V. 2005 Natural layer-by-layer photonic structure in the squamae of *Hoplia coerulea* (Coleoptera). Phys. Rev. E 72, 061904. (doi:10.1103/PhysRevE.72.061904)

51. Deparis O, Mouchet SR, Dellieu L, Colomer JF, Sarrazin M. 2014 Nanostructured surfaces: Bioinspiration for transparency, coloration and wettability. Mater. Today Proc. 1S, 122-129. (doi:10.1016/j.matpr.2014.09.008)

52. Vukusic P, Sambles JR, Lawrence CR, Wootton RJ. 1999 Quantified interference and diffraction in single *Morpho* butterfly scales. Proc. R. Soc. Lond. B 266, 1403-1411. (doi:10.1098/rspb.1999.0794)

53. Sollas IBJ. 1907 On the Identification of Chitin by Its Physical Constants. Proc. R. Soc. Lond. B 79, 474-484. (doi:10.1098/rspb.1907.0042)

54. Berthier S, Charron E, Da Silva A. 2003 Determination of the cuticle index of the scales of the iridescent butterfly *Morpho menelaus*. Opt. Commun. 228, 349-356. (doi:10.1016/j.optcom.2003.10.032)

55. Leertouwer HL, Wilts BD, Stavenga DG. 2011 Refractive index and dispersion of butterfly chitin and bird keratin measured by polarizing interference microscopy. Opt. Express 19, 24061-24066. (doi:10.1364/OE.19.024061)

56. Yoshioka S, Kinoshita S. 2011 Direct determination of the refractive index of natural multilayer systems. Phys. Rev. E 83, 051917. (doi: 10.1103/PhysRevE.83.051917)

57. Yeh P. 2005 Optical Waves in Layered Media. Wiley-Interscience, Hoboken.

58. Taflove A, Hagness SC. 2000 Computational Electrodynamics: The Finite-Difference Time-Domain Method. Artech, Norwood.

59. Oskooi AF, Roundy D, Ibanescu M, Bermel P, Joannopoulos JD, Johnson SG. 2010 MEEP: A flexible free-software package for electromagnetic simulations by the FDTD method. Comp. Phys. Commun. 181, 687-702. (doi:10.1016/j.cpc.2009.11.008)

572 60. Vandenbem C. 2006 Contribution à l'étude de la réflectance et du confinement des
573 modes dans les systèmes optiques stratifiés. Ph.D. thesis - Facultés Universitaires Notre-
574 Dame de la Paix (FUNDP), Namur.
575 61. Nikolaev IS, Vos WL, Koenderink AF. 2009 Accurate calculation of the local density of
576 optical states in inverse-opal photonic crystal. J. Opt. Soc. Am. B 26, 987-997.
577 (doi:10.1364/JOSAB.26.000987)
578 62. Deparis O, Vandenbem C, Rassart M, Welch VL, Vigneron JP. 2006 Color-selecting
579 reflectors inspired from biological periodic multilayer structures. Opt. Express 14, 3547-3555.
580 (doi:10.1364/OE.14.003547)
581 63. Barnes WL. 1998 Fluorescence near interfaces: the role of photonic mode density. J.
582 Modern Opt. 45, 661-699. (doi:10.1080/09500349808230614)
583 64. Kolaric B, Desprez S, Brau F, Damman P. 2012 Design of curved photonic crystal using
584 swelling induced instabilities. J. Mater. Chem. 22, 16205-16208. (doi:10.1039/C2JM32997B)
585

Figure 1 The male *H. coerulea* beetle displays a vivid violet-blue iridescent colour (a) due to a porous multilayer structure located in the scales covering its elytra and thorax. The photonic structure is a periodic stack of thin pure cuticle layers and mixed air-cuticle porous layers (b,c). In the structural model used for simulations, the layers comprising a mixture of air (in the pores) and cuticle material (associated with the rods) were approximated by homogeneous layers with an effective refractive index (RI) (d).

Figure 2 Colour and fluorescence changes of the scales of the male *H. coerulea* beetle induced by contact with water. Illuminated by visible white light (at normal incidence and detection), the beetle scales appear violet-blue in the dry state (a) and green in the wet state (b). The reflectance peak wavelength shifts from 458 nm to 525 nm when the elytron is in contact with water (c). Under UV light (with a 45° incidence and detection angle), the scales produce a turquoise coloured emission in the dry state (d) and a dark blue colour in the wet state (e). Where scales overlap, the fluorescence intensity is higher. This effect is due to the transparency of the scales at the emitted wavelengths. Although there is almost no water-induced change in the excitation spectrum peak wavelength and its associated FWHM, the emission spectrum peak wavelength shifts from 463 nm to 446 nm when the elytron is in contact with water. The associated FWHM reduces from 121 nm to 105 nm (f).

Figure 3 Reflectance spectra calculated for the modelled photonic structure of a male *H. coerulea* beetle (Figure 1c) using unpolarised light at normal incidence. The reflectance peak centre wavelength shifts from 461 nm to 501 nm when the structure changes from dry (blue curves) to wet (green curve) state and the reflectance peak intensity decrease (a). The related photonic band structure and density of optical states (DOS) are also modified accordingly (b and c). The reflectance peak widths and the PhBG widths decrease in the wet state.

Figure 4 When the pores of the modelled photonic structure are filled with water, the peak emission wavelength shifts from 480 nm to 428 nm (a) and from 429 nm to 416 nm (b) in the cases of both investigated models. a) In the first model, emitting planar sources are assumed to be located in the different pure cuticle layers of the photonic structure. The presented spectra result from the averages over 12 simulated spectra that individually correspond to fluorophores located in each of the 12 pure cuticle layers. b) In the second model, the fluorophores are assumed to be 180 point sources distributed across the photonic structure.

612

	Dry state		Wet state	
Emission wavelength (nm)	Decay time τ (ns)	Standard error (SE) (ns)	Decay time τ (ns)	Standard error (SE) (ns)
466	3.9	0.55	1.4	0.04
	0.79	0.02		
546	1.9	0.05	1.4	0.04

613 **Table 1** Decay times and the related standard errors of the fluorophores embedded in *H. coerulea* beetle's scales in both dry
614 and wet states inside (466 nm) and outside (546 nm) the PhBG of the structure. The incident light formed a 45° angle with the
615 direction normal to the sample surface, with a wavelength equal to 376 nm. The emitted light was detected at a 45° angle on the
616 other side of the normal direction.

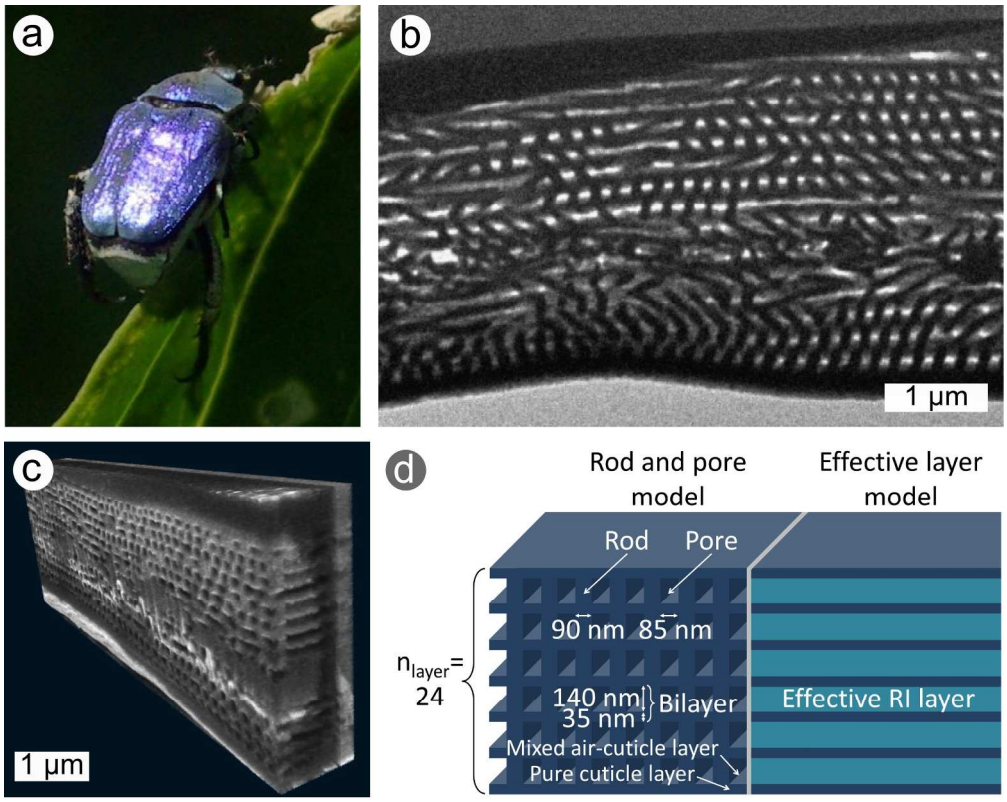

The male *H. coerulea* beetle displays a vivid violet-blue iridescent colour (a) due to a porous multilayer structure located in the scales covering its elytra and thorax. The photonic structure is a periodic stack of thin pure cuticle layers and mixed air-cuticle porous layers (b,c). In the structural model used for simulations, the layers comprising a mixture of air (in the pores) and cuticle material (associated with the rods) were approximated by homogeneous layers with an effective refractive index (RI) (d).

Figure 1
527x417mm (120 x 120 DPI)

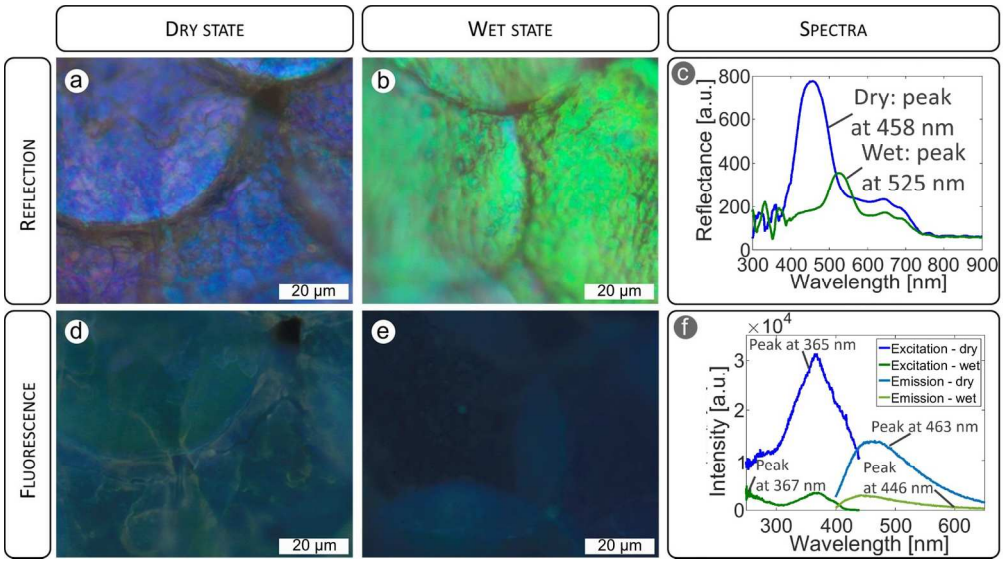

Colour and fluorescence changes of the scales of the male *H. coerulea* beetle induced by contact with water. Illuminated by visible white light (at normal incidence and detection), the beetle scales appear violet-blue in the dry state (a) and green in the wet state (b). The reflectance peak wavelength shifts from 458 nm to 525 nm when the elytron is in contact with water (c). Under UV light (with a 45° incidence and detection angle), the scales produce a turquoise coloured emission in the dry state (d) and a dark blue colour in the wet state (e). Where scales overlap, the fluorescence intensity is higher. This effect is due to the transparency of the scales at the emitted wavelengths. Although there is almost no water-induced change in the excitation spectrum peak wavelength and its associated FWHM, the emission spectrum peak wavelength shifts from 463 nm to 446 nm when the elytron is in contact with water. The associated FWHM reduces from 121 nm to 105 nm (f).

Figure 2
401x222mm (120 x 120 DPI)

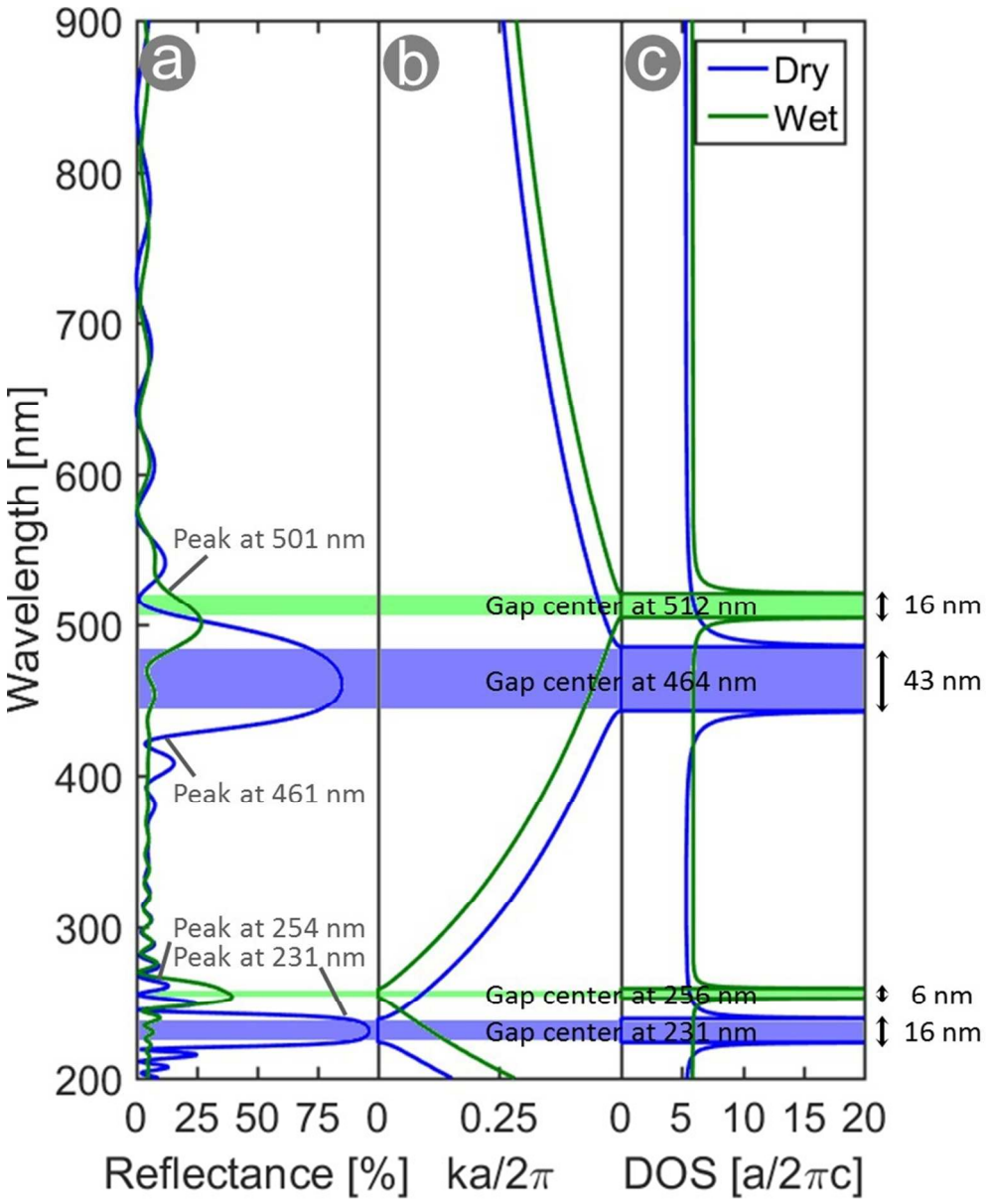

Reflectance spectra calculated for the modelled photonic structure of a male *H. coerulea* beetle (Figure 1c) using unpolarised light at normal incidence. The reflectance peak centre wavelength shifts from 461 nm to 501 nm when the structure changes from dry (blue curves) to wet (green curve) state and the reflectance peak intensity decrease (a). The related photonic band structure and density of optical states (DOS) are also modified accordingly (b and c). The reflectance peak widths and the PhBG widths decrease in the wet state.

Figure 3
194x237mm (120 x 120 DPI)

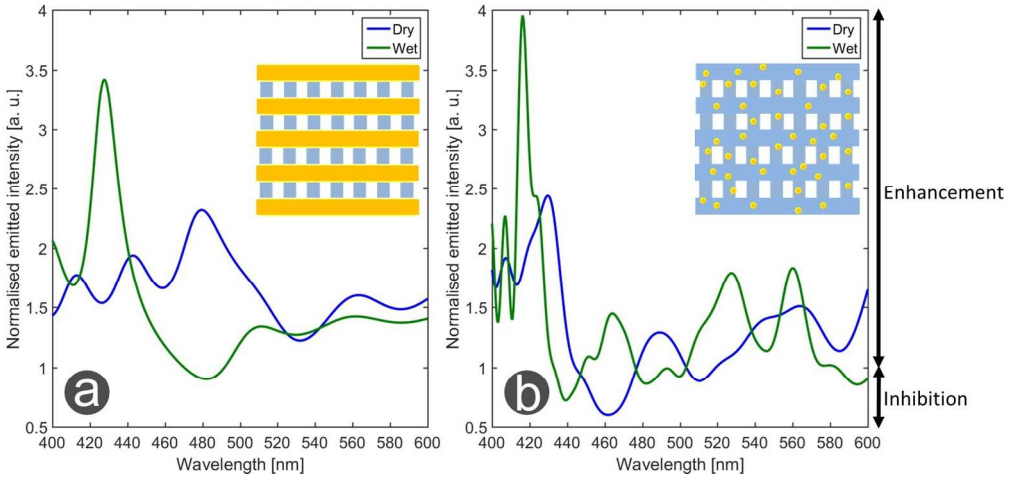

When the pores of the modelled photonic structure are filled with water, the peak emission wavelength shifts from 480 nm to 428 nm (a) and from 429 nm to 416 nm (b) in the cases of both investigated models. a) In the first model, emitting planar sources are assumed to be located in the different pure cuticle layers of the photonic structure. The presented spectra result from the averages over 12 simulated spectra that individually correspond to fluorophores located in each of the 12 pure cuticle layers. b) In the second model, the fluorophores are assumed to be 180 point sources distributed across the photonic structure.

Figure 4
375x179mm (120 x 120 DPI)